

<https://doi.org/10.1038/s43856-025-00990-9>

Cognitive characteristics and ischemic prognosis of quantitative white matter hyperintensities in adult moyamoya disease

Check for updates

Ziqi Liu^{1,6}, Xiaokuan Hao^{1,6}, Qi Duan², Chaoran Shen³, Haojin Lyu², Junze Zhang¹, Jing Gu¹, Shihao He^{1,4}, Yanru Wang¹, Xilong Wang¹, Zhenyu Zhou¹, Ning Ma¹, Ran Duan⁵, Xinlin Zhou³, Xin Lou² ✉ & Rong Wang¹ ✉

Abstract

Background White matter hyperintensities (WMHs) are associated with long-term stroke and cognitive decline in the elderly population but differ from the young and middle-aged populations, especially for those with moyamoya disease (MMD). The aim of this study was to modify the Fazekas grade and quantitatively analyze the effects of WMHs on multiple cognitive domains and 2-year clinical ischemic events in adult MMD patients.

Methods Adult MMD patients and healthy controls were recruited for a comprehensive cognitive assessment. Among 151 adult MMD patients, the average age was 41.78 ± 10.59 years and the male-to-female ratio was 0.94. Adjusted quantitative whole-brain, periventricular (PVWMHs), and deep WMHs (DWMHs) were included in the proportional hazards model to explore their relationships with 2-year ischemic events. Linear regression analysis was used to evaluate the correlation between the WMH burden in different brain regions and various cognitive domains.

Results MMD patients present decreases in intelligence ($P = 0.000$), spatial working memory ($P = 0.011$), verbal working memory 1 ($P = 0.000$) and 2 ($P = 0.000$), mental rotation ($P = 0.008$), and executive inhibition ($P = 0.011$). Quantitative whole-brain \log_{10} WMHs (adjusted HR = 6.757, $P = 0.001$) and \log_{10} PVWMHs (adjusted HR = 8.824, $P = 0.000$) are independently associated with future ischemic events. The area under curve (AUC) of the quantitative PVWMH for the prediction of 2-year ischemic events is 0.701, which is better than that of the Fazekas grade (AUC = 0.561) ($P = 0.000$).

Conclusions PVWMHs have greater potential effects on verbal working memory, attention, and simple subtraction in adult MMD patients when compared with DWMHs. An increase in PVWMHs could be an indicator of future ischemic events in adults with MMD.

Clinical registration Clinical registration no. ChiCTR2200058251 URL: <https://www.chictr.org.cn/>.

Plain language summary

The increase in white matter hyperintensities (WMH), or lesions in the brain, is a common factor leading to cognitive decline and ischemic stroke events during the aging process. The association between WMH in moyamoya disease, a rare blood vessel disorder, remains unclear. This study focuses on the potential association between the increased WMH in people with moyamoya disease and their cognitive functions. Through measurable analysis of WMH, the authors found that an increase in a specific type of WMH, the periventricular region of the brain, was associated with certain cognitive declines. An increase in periventricular WMH beyond a certain threshold can therefore lead to an increase in long-term ischemic events such as transient neurological deficits and strokes.

¹Department of Neurosurgery, Beijing Tiantan Hospital, Capital Medical University, Beijing, China. ²Department of Radiology, Chinese PLA General Hospital, Beijing, China. ³State Key Laboratory of Cognitive Neuroscience and Learning, Beijing Normal University, Beijing, China. ⁴Department of Neurosurgery, Peking Union Medical College Hospital, Beijing, China. ⁵Department of Neurosurgery, Peking University International Hospital, Beijing, China. ⁶These authors contributed equally: Ziqi Liu, Xiaokuan Hao. ✉ e-mail: louxin@301hospital.com.cn; ronger090614@ccmu.edu.cn

White matter hyperintensities (WMHs), which are widespread in the elderly population¹, have been shown to be associated with long-term stroke and cognitive decline^{2,3}. The pathological mechanism is thought to be related to the occlusion of small vessels. For young and middle-aged adults, however, studies on whether increased WMHs are related to further stroke and cognitive dysfunction are still lacking.

Most previous studies have distinguished WMHs according to the Fazekas grade (1987)⁴. This classical grade can qualitatively describe the range and distribution of WMHs but cannot quantitatively localize the effects of WMHs on the prognosis of further ischemic events and cognitive dysfunction². Several studies have shown that the strategic location of the lesion is a better predictor of cognitive outcome than the general WMH volume is, and voxel-based quantitative analysis is better able to investigate the effects of local WMHs^{5,6}. Therefore, we designed a more accurate method to quantitatively study WMHs in moyamoya disease (MMD) patients, and then, we applied a well-established quantitative WMH measure to investigate its association with multiple cognitive domains and predict future ischemic outcomes in MMD patients. MMD is a vascular disease that spans childhood, youth, middle age, and old age and is characterized by progressive transient ischemic attack (TIA), stroke and cognitive dysfunction^{7,8}. Our previous study revealed that white matter microdamage in MMD patients plays an important role in cognitive decline^{9,10}. For one thing, WMH volume can lead to decreases in executive function, short-term memory and reactions; in addition, there is a consistent positive correlation between WMHs and further ischemic events¹¹. WMHs in MMD patients are usually found in the periventricular watershed¹², which is consistent with the underlying mechanism of WMHs¹³. However, whether different degrees and locations of WMHs can affect cognitive domains in young and middle-aged patients is still unknown, and further survival analyses on ischemic events need to be performed to identify a WMH marker and its cutoff value to guide potential future treatment strategies.

The hemisphere affected by MMD is generally considered hypoperfused, even in nonstroke patients. With the hypoperfusion model from MMD^{14,15}, we study the quantitative burden of WMHs on cognitive function and the long-term prognosis of ischemia in young and middle-aged MMD patients. We hypothesize that quantitative WMH analysis can provide a potential clinical WMH threshold, which can modify the traditional Fazekas grade to improve treatment strategies and provide evidence for potential further ischemic risk with increased WMHs in MMD patients. The secondary aim is to explore whether there is a correlation between WMHs and cognitive decline.

In this study, we find the effects of WMHs on cognitive function are selective in MMD. Comparing PVWMHs with DWMHs, PVWMHs have greater potential effects on verbal working memory, attention, and simple subtraction. Therefore, PVWMHs could be a more sensitive indicator for future ischemic events in adult MMD patients.

Methods

Study population

The clinical data of consecutive patients who attended Beijing Tiantan Hospital, People's Liberation Army (PLA) General Hospital and Peking University International Hospital from 04/01/2018 to 06/01/2024 were prospectively collected according to the following criteria. Among the 151 participants, the average age was 41.78 ± 10.59 years, the average education level was 11.95 ± 4.19 years, and the male-to-female ratio was 0.94.

Inclusion criteria

(1) Diagnosis based on digital subtraction angiography or magnetic resonance angiography according to the guidelines¹⁶. (2) Education age ≥ 3 years and ability to use cognitive testing equipment. (3) Age ≥ 18 years and ≤ 60 years. (4) Modified Rankin scale (mRS) score ≤ 1 . (5) Magnetic resonance

imaging (MRI) was performed with both 3D-T1 and fluid-attenuated inversion recovery (FLAIR) sequences.

Exclusion criteria

(1) Severe movement disorders, language disorders, aphasia, hemianopsia or hemiplegia. (2) Hamilton Anxiety Scale score >7 or Hamilton Depression Scale score >8 . (3) Inability to complete follow-up. (4) Neurological deficits due to psychiatric disorders and severe systemic illness. (5) Poor quality of MRI scans, which could affect subsequent registration and quantification. (6) Structural lesions (lacunar cerebral infarction >8 mm in maximum diameter, cerebral hemorrhage, or other substantial lesions, such as brain tumors and metal bodies) that could affect the automatic segmentation process on MRI scans.

Inclusion and exclusion criteria for the control group

Inclusion criteria for the control group. (1) Education age ≥ 3 years, ability to use cognitive testing equipment. (2) Age ≥ 18 years old and ≤ 60 years old. (3) mRS score ≤ 1 . (3) No history of stroke and no lacunar cerebral infarction >8 mm in maximum diameter, cerebral hemorrhage, or other substantial lesions, such as brain tumors or metal bodies on MRI scans.

Exclusion criteria for the control group. (1) Severe movement disorders, language disorders, aphasia, hemianopsia or hemiplegia. (2) Hamilton Anxiety Scale score >7 or Hamilton Depression Scale score >8 . (3) Neurological deficits due to psychiatric disorders or severe systemic illness.

Ethics approval and consent to participate

The study was performed according to the guidelines of the Declaration of Helsinki and approved by the research ethics committee of Beijing Tiantan Hospital affiliated with Capital Medical University (KYSQ 2019-058-01, KY2022-032-03). Written informed consent for publication was obtained from all participants.

Neuropsychological assessment

All the neuropsychological assessment tasks were web-based and are available at www.dweipsy.com/lattice^{17,18}. The tests on this platform are scored automatically, which avoids potential subjective bias. The participants completed the tests at a computer workstation under the guidance of the same neuropsychologist at each center who was unaware of the clinical information.

The interval between neuropsychological testing and MRI scans was 14 days or less. The cognitive tests included 16 cognitive domains. Details about the cognitive assessments can be found in the Supplementary File Supplementary Method 1.

MRI acquisition and processing

The images were acquired using 3D-T1-weighted (magnetization-prepared rapid gradient echo [MPRAGE], fast spoiled gradient echo [FSPGR]) and T2-weighted fluid-attenuated inversion recovery (FLAIR) sequences using a 3 T scanner (Philips Medical Systems, Best, The Netherlands [$N = 112$] or Discovery MR750W, GE Medical Systems, USA [$N = 39$]). The scanning parameters were set as follows:

FLAIR sequence. Repetition time (TR) = 4800 (8500) ms. Echo time (TE) = 256 (166) ms. Inversion time (TI) = 1650 (2100) ms. Flip angle = 90 (111) $^\circ$, matrix size = 220 (288) \times 218 (224), field of view (FOV) = 220 (288) \times 218 (224), yielding $1 \times 1 \times 1$ mm³ voxels. Slice thickness = 1 mm without a gap.

3D-T1-weighted MPRAGE sequence. TR = 6.36 ms, TE = 3.04 ms, flip angle = 15° , matrix size = 256×256 , slice thickness = 1 mm without a gap, and FOV = 256×256 , yielding $1 \times 1 \times 1$ mm³ voxels.

3D-T1-weighted FSPGR sequence. TR = 7.0 ms, TE = 2.96 ms, flip angle = 8° , matrix size = 220×218 , slice thickness = 1 mm without a gap, and FOV = 220×218 , yielding $1 \times 1 \times 1$ mm³ voxels.

The intracranial volume (ICV) and WMH volume were automatically extracted from 3D-T1 and FLAIR images. In addition, individual 3D-T1 images were segmented into cerebrospinal fluid (CSF), white matter (WM) and gray matter (GM) via Statistical Parametric Mapping 12 (SPM12). The ICV estimate was obtained by multiplying the sum of the probabilities of voxels belonging to each tissue class by the volume of the voxel in the 3D-T1 image ($1 \times 1 \times 1 \text{ mm}^3$). WMH volumes were calculated with the UBO Detector (<https://cheba.unsw.edu.au/group/neuroimagingpipeline>), a fully automated toolbox for extracting WMHs¹⁹. First, the FLAIR image was registered to the corresponding 3D-T1 image. The 3D-T1 images were then warped to the diffeomorphic anatomical registration through exponentiated lie (DARTEL) space²⁰. Next, the resulting field maps were applied to warp the FLAIR images that were registered to the 3D-T1 images to the same DARTEL space¹⁹. After removing nonbrain and inhomogeneous tissues on FLAIR in DARTEL space, WMH and nonWMH tissues were classified with a k-nearest neighbor (k-NN)-based algorithm¹⁹. DWMHs were defined as WMH voxels in DARTEL space that were 12 mm away from the periventricular mask, and the remaining WMH voxels were defined as PVWMHs¹⁹. Like the present study, many previous studies have used 12 mm as the threshold to segment PVWMHs and DWMHs^{19,21}. All volume calculations were performed using standard Montreal Neurosciences Institute (MNI152) 1 mm^3 brain templates to control the ICV effect on the WMH volumes.

Statistics and reproducibility

All the statistical analyses were performed with Statistical Package for the Social Sciences (20.0). Pearson's chi-square test was used to compare categorical variables. The skewness, peakedness, histogram and quantile-quantile plot were used to test the normality of the data distribution. All the data were statistically analyzed for reliability, and a Guttman's half coefficient ≥ 0.70 was considered reliable. A Cronbach's alpha ≥ 0.70 was considered to indicate good internal consistency. Multiple linear regression was used to adjust for demographic factors, such as age, sex, and education level, that were associated with each cognitive domain. Adjusted R^2 and regression coefficients (β) were used to assess the contributions of different brain regions to each cognitive domain. Independent sample t tests were used to compare cognitive function between MMD patients and controls. One-way analysis of variance (ANOVA) and post hoc tests were used to analyze the differences in cognitive function between subgroups. Subgroup analyses were performed based on the side of the moyamoya hemisphere (left, right, and bilateral) to explore the effects of different moyamoya hemisphere sides on multiple cognitive domains. Linear regression models with the covariates were used to examine the associations of different lobe regions in the left or right hemisphere with multiple cognitive domains. The Bonferroni correction method was used for post hoc tests. Adjusted P (Bonferroni correction) = P values \times compared times or $\alpha_{\text{corrected}} = \alpha_{\text{uncorrected}} \div$ compared times. Receiver operating characteristic (ROC) curves were used to measure the ability of quantitative WMH or Fazekas grade⁴ to distinguish future ischemic events. The Delong test was used to detect differences between quantitative and qualitative WMH assessments, and then the maximum Youden index was calculated to determine the optimal cutoff values. According to the cutoff values of quantitative WMHs, MMD patients were divided into 2 groups (Q1, volume <cutoff value; Q2, volume >cutoff value) to examine whether whole-brain WMHs, PVWMHs and DWMHs had different clinical prognostic effects on the occurrence of ischemic events with increasing WMHs. The proportional hazards (PH) assumption was tested to guarantee the precondition of Cox regression.

The Cox proportional hazards model was used for survival analysis after MRI to evaluate the hazard ratios (HRs) of ischemic event occurrence on the basis of the WMH distribution. Age, sex, education, smoking history, long-term alcohol use and medical comorbidities were included in the model as covariables to adjust for different patterns of WHMs.

Continuous data are presented as the means \pm standard deviations. The level of significance was set at a two-sided P value < 0.05 . Power analysis was used to calculate power according to effect size, sample size and two-

sided α ($\alpha = 0.05$) in Power Analysis and Sample Size Software (2017; NCSS, LLC, Kaysville, Utah, USA, <https://ncss.com/software/pass>). The power < 0.80 may lead to an increased probability of making a type II error and were considered to be unreliable.

Results

Participant demographic information

A total of 154 patients from 3 medical centers were initially enrolled in the study. Among them, one patient had poor image quality, and 2 patients had a Hamilton Depression Scale score > 8 . Ultimately, a total of 151 individuals were included in the analysis after exclusion. Seventy-seven healthy controls matched for age, sex, and education level were also included to compare cognitive function.

Among the 151 participants, the average age was 41.78 ± 10.59 years, the average education level was 11.95 ± 4.19 years, and the male-to-female ratio was 0.94. A total of 100 patients were diagnosed with bilateral MMD, 25 with right MMD, and 26 with left MMD. The mean follow-up period was 24.74 ± 15.84 months. No patients were lost to follow-up.

Details of the patients in the MMD group and the control group are shown in Table 1.

Cognitive function domain comparison

Compared with the control group, the MMD group exhibited decreased function in the intelligence ($P = 0.000$), spatial working memory ($P = 0.011$), verbal working memory 1 ($P = 0.000$) and 2 ($P = 0.000$), mental rotation ($P = 0.008$), and executive inhibition ($P = 0.011$) domains. No significant differences were found in the other 10 cognitive function domains. Table 1 displays the details of the cognitive data.

One-way ANOVA revealed that cognitive impairment was more significant in MMD patients with left hemisphere involvement, especially impairments in intelligence and verbal working memory. There was no significant difference in cognitive function between the MMD patients with right hemisphere involvement alone and the control group. Figure 1A–P shows the details of the cognitive data.

Correlation analysis between WMHs and cognitive domains

With linear regression after adjusting for age and education, we found that whole-brain WMHs were significantly associated with executive control ($\beta = -0.232$, $P = 0.041$; $\beta = -0.256$, $P = 0.024$) and executive inhibition ($\beta = -0.200$, $P = 0.032$), while PVWMHs were associated with verbal working memory ($\beta = -0.185$, $P = 0.031$; $\beta = -0.206$, $P = 0.017$) and executive control ($\beta = -0.280$, $P = 0.015$). DWMHs were associated only with word memory ($\beta = -0.172$, $P = 0.036$) and executive inhibition ($\beta = -0.226$, $P = 0.015$). However, after adjusting for multiple comparisons, no cognitive function was significantly. Additional information from this analysis is presented in Table 2.

After further partitioning, word memory was significantly correlated with the left occipital lobe ($\beta = -0.300$, $P = 0.000$). Verbal working memory in order ($\beta = -0.199$, $P = 0.021$), simple subtraction ($\beta = -0.251$, $P = 0.025$), executive function in the same direction ($\beta = -0.252$, $P = 0.026$) and executive inhibition ($\beta = -0.260$, $P = 0.008$) were significantly correlated with the left frontal lobe. Executive inhibition was significantly correlated with the left parietal lobe ($\beta = -0.222$, $P = 0.016$). Word memory was significantly correlated with the left occipital lobe ($\beta = -0.300$, $P = 0.000$).

Additional information from this analysis is presented in Supplementary Data 1, Supplementary Table 1, and Supplementary Fig. 1.

Fazekas grade and quantitative WMH

The primary outcome was defined as ischemic event (ischemic stroke + TIA). The area under the curve (AUC) of the Fazekas grade (PVWMH) was 0.561, whereas the AUC of the quantitative PVWMH was 0.701. The AUC of the Fazekas grade (DWMH) was 0.542, whereas the AUC of the quantitative DWMH was 0.604 ($P = 0.035$). The AUC of the Fazekas grade (WMH) was 0.567, whereas the AUC of the quantitative whole-brain WMH score was 0.666. The Delong test revealed significant differences between the

Table 1 | Demographic characteristics and cognitive function

Variables	N (MMD/HC)	MMD-G	HC-G	P values	Adjusted P values
Age (years)	151/77	41.78 ± 10.59	39.46 ± 13.59	0.190	NA
Sex (M:F)	151/77	0.94	0.88	0.820	NA
Education (years)	151/77	11.95 ± 4.19	12.83 ± 3.61	0.100	NA
Comorbidities	151/77	NA	NA	NA	NA
Hypertension	151/77	26 (17.2%)	11 (14.3%)	0.570	NA
Diabetes	151/77	11 (7.3%)	0 (0%)	0.018	NA
Hyperlipidemia	151/77	22 (14.6%)	10 (13%)	0.745	NA
Thyroid disorder	151/77	7 (4.6%)	0 (0%)	0.098	NA
Coronary heart disease	151/77	1 (0.7%)	0 (0%)	1.000	NA
Immune disease	151/77	2 (1.3%)	1 (1.3%)	1.000	NA
Smoke history	151/77	12 (7.9%)	4 (5.2%)	0.442	NA
Long-term alcohol use	151/77	3 (2.0%)	3 (3.9%)	0.408	NA
CRT ^a	148/77	470.56 ± 142.28	477.00 ± 161.01	0.759	12.144
RAVEN	87/68	17.55 ± 5.33	21.50 ± 7.67	0.000*	0.004*
ROTATION	43/48	16.07 ± 8.38	21.29 ± 9.93	0.008*	0.128
SWM	63/24	80.49 ± 5.35	83.63 ± 3.90	0.011*	0.176
VWM1	148/72	7.84 ± 1.57	8.25 ± 2.44	0.000*	0.000*
VWM2	147/70	5.96 ± 1.78	7.37 ± 2.52	0.000*	0.001*
SUBTRACT	83/72	43.8 ± 8.86	45.06 ± 10.04	0.408	6.528
COMSUB	84/69	21.83 ± 7.87	23.22 ± 8.22	0.290	4.640
WORDM	146/76	61.92 ± 13.69	64.34 ± 12.74	0.203	3.248
PICTM ^a	44/72	72.91 ± 11.97	72.83 ± 8.73	0.969	15.504
EXCUT1 ^a	84/36	43.62 ± 22.86	43.42 ± 24.00	0.965	15.440
EXCUT2 ^a	84/36	43.76 ± 22.42	42.64 ± 23.21	0.804	12.864
Number comparison	105/25	78.34 ± 6.43	80.40 ± 3.56	0.126	2.016
Visual tracing	103/26	15.48 ± 8.85	13.54 ± 6.85	0.301	4.816
Figure matching	105/25	63.48 ± 25.77	71.80 ± 20.07	0.134	2.144
GO/NO GO	106/26	83.82 ± 19.98	94.04 ± 6.89	0.011*	0.176

Adjusted P values (Bonferroni correction) = P values × compared times (16). $\alpha_{corrected} = 0.05 \div \text{compared times (16)} = 0.003125$.

CRT choice reaction time, RAVEN Raven's standard progressive matrices, ROTATION mental rotation, SWM spatial working memory, VWM1 verbal working memory, recite in order, VWM2 verbal working memory, recite in reverse order, SUB simple subtraction, COMSUB complex subtraction, WORDM word memory, PICTM picture memory, EXCUT1 executive function, same direction, EXCUT2 executive function, opposite direction, MMD-G moyamoya disease group, HC-G healthy control group, N number.

*P values <0.05.

^aThe power was <0.8.

quantitative PVWMH grade and periventricular Fazekas grade ($P = 0.000$, adjusted $P = 0.001$). The maximum Youden index was 0.359 (specificity = 0.667 and sensitivity = 0.692) when the cutoff of PVWMHs was 4280 mm³ according to MNI152 standard brain mapping.

Additional information from this analysis is presented in Fig. 2 and Supplementary Tables 2 and 3.

Cox regression and Kaplan–Meier curve analyses of WMHs and ischemic events

Among the 151 MMD patients with medical follow-up data, 2 ischemic strokes and 50 TIAs occurred during the follow-up period.

Based on the cutoff value, the patients were divided into Q1 (<cutoff value) and Q2 (>cutoff value) groups for Cox regression after adjustment. PVWMHs >4280 mm³ (HR = 3.737 [95% CI, 1.959–7.127], $P = 0.000$) were independently associated with long-term ischemic events. Similar results were also observed for whole-brain WMHs and DWMHs. Additional information from this analysis is presented in Fig. 2.

Quantitative WMHs after log transformation showed similar results. Log₁₀Whole-brain WMHs (adjusted HR = 6.757 [95% CI, 2.274–20.075]; $P = 0.001$) and log₁₀PVWMHs (adjusted HR = 8.824 [95% CI, 3.039–25.620]; $P = 0.000$) remained an independent risk factor for future

ischemic events, while log₁₀DWMHs (adjusted HR = 2.605 [95% CI, 1.144–5.929]; $P = 0.023$) had potential predictive value, but its effect needs to be further clarified.

Additional information from this analysis is presented in Fig. 2 and Table 3.

Discussion

In this study, by investigating the outcome of 2-year ischemic events with quantitative WMHs, a sequential increase in PVWMHs was found to be an independent risk factor for future ischemic events. A PVWMH exceeding 4280 mm³ was the optimal threshold. Moreover, we found that a decrease in multiple cognitive functions was associated with an increase of WMHs, especially PVWMHs, in young and middle-aged MMD patients. In addition, MMD with left hemisphere involvement was more likely to lead to a decline in intelligence, working memory and executive function.

Compared with the qualitative Fazekas grade, the quantitative WMH had a greater ability to predict the prognosis of MMD patients. In a previous study, quantitative and qualitative WMH assessments were highly correlated and comparable in older patients²². WMH burden is associated with short-term outcomes in patients with good prestroke function in the presence of intracranial stenosis/occlusion.

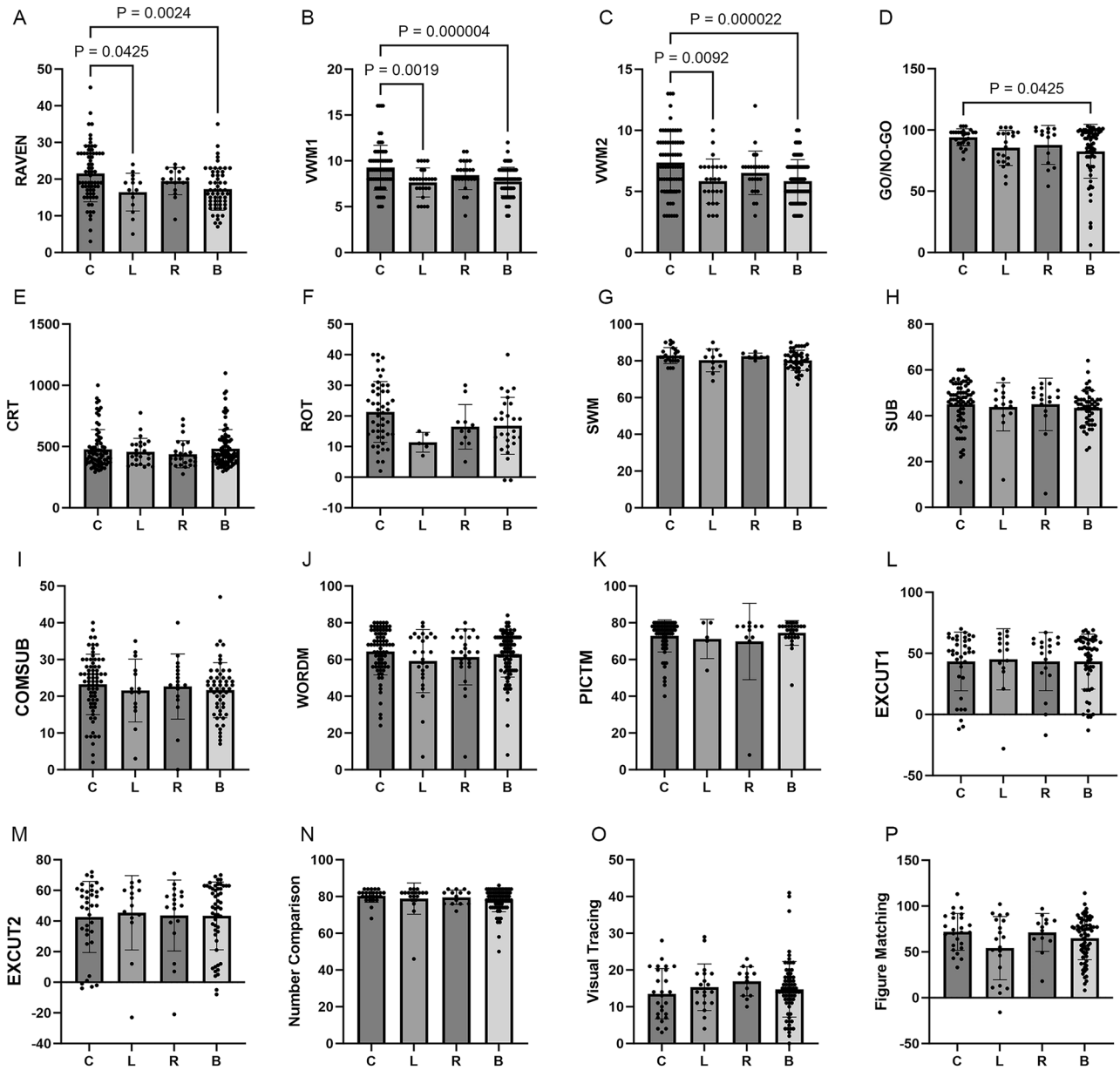


Fig. 1 | One-way ANOVA results of cognitive function for healthy controls (C) and patients with left (L), right (R), and bilateral (B) MMD with Bonferroni correction. **A** RAVEN = Raven's Standard Progressive Matrices, $N = 68$ (C)/15 (L)/17 (R)/55 (B); **B** VWM1 = verbal working memory, recite in order, $N = 72$ (C)/25 (L)/25 (R)/98 (B); **C** VWM2 = verbal working memory, recite in reverse order, $N = 70$ (C)/25 (L)/25 (R)/97 (B); **D** GO/NO GO, $N = 26$ (C)/20 (L)/14 (R)/72 (B); **E** CRT = choice reaction time, $N = 77$ (C)/24 (L)/25 (R)/99 (B); **F** ROT = mental rotation, $N = 48$ (C)/5 (L)/11 (R)/27 (B); **G** SWM = spatial working memory, $N = 24$ (C)/11 (L)/7 (R)/45 (B); **H** SUB = simple subtraction, $N = 72$ (C)/14 (L)/17 (R)/52 (B); **I** COMSUB= complex subtraction, $N = 69$ (C)/14 (L)/17 (R)/53 (B); **J** WORDM = word memory, $N = 76$ (C)/25 (L)/25 (R)/96 (B); **K** PICTM = picture memory, $N = 72$ (C)/5 (L)/11 (R)/28 (B); **L** EXCUT1 = executive function, same direction, $N = 36$ (C)/14 (L)/18 (R)/52 (B); **M** EXCUT2 = executive function, opposite direction, $N = 36$ (C)/14 (L)/18 (R)/52 (B). **N** Number comparison, $N = 25$ (C)/19 (L)/14 (R)/72 (B); **O** Visual tracing, $N = 26$ (C)/19 (L)/13 (R)/71 (B); **P** Figure matching, $N = 25$ (C)/20 (L)/13 (R)/72 (B). Error bars are mean \pm SD.

(B); **I** COMSUB= complex subtraction, $N = 69$ (C)/14 (L)/17 (R)/53 (B); **J** WORDM = word memory, $N = 76$ (C)/25 (L)/25 (R)/96 (B); **K** PICTM = picture memory, $N = 72$ (C)/5 (L)/11 (R)/28 (B); **L** EXCUT1 = executive function, same direction, $N = 36$ (C)/14 (L)/18 (R)/52 (B); **M** EXCUT2 = executive function, opposite direction, $N = 36$ (C)/14 (L)/18 (R)/52 (B). **N** Number comparison, $N = 25$ (C)/19 (L)/14 (R)/72 (B); **O** Visual tracing, $N = 26$ (C)/19 (L)/13 (R)/71 (B); **P** Figure matching, $N = 25$ (C)/20 (L)/13 (R)/72 (B). Error bars are mean \pm SD.

A previous study reported that among patients with MMD who had PVWMHs, 2.12% (2/94) experienced stroke during a 3-year follow-up, with a mean annual risk of ischemic stroke of 0.69%¹¹. This risk is much lower than the risk of natural stroke onset among asymptomatic patients (average annual ischemic stroke risk 0.19–1.09%)^{23,24}. Two strokes (2/151) and 50 TIAs (50/151) were observed in this study during the 2-year follow-up period (average annual ischemic stroke risk 0.66%), which is consistent with the results of previous studies. PVWMHs may be an independent risk factor for TIA and stroke in MMD patients. However, further controlled experiments are needed to confirm these results.

MMD patients without stroke retain most of their normal cognitive function. However, intelligence, mental rotation, spatial working memory, verbal working memory and executive inhibition are still impaired. Previous studies have shown that cognitive impairment in MMD patients is selective, especially in intelligence, mental rotation, and short-term memory, regardless of ischemic stroke status^{9,10}. White matter damage may play an important role in impairments in executive function, attention, and working memory¹⁴. Previous studies of MMD patients without stroke have also identified executive function, mental efficiency, and word finding as the most commonly impaired domains, whereas memory is relatively intact²⁵. However, some studies have argued that global cognition (MoCA),

Table 2 | Linear regression for WMH regions associated with different cognitive domains

Variables ^a	Whole-brain WMH					PVMMH					DWMH				
	R ²	P (F)	β	P	Adjusted P	R ²	P (F)	β	P	Adjusted P	R ²	P (F)	β	P	Adjusted P
CRT	0.071	0.013	0.002	0.985	15.760	0.044	0.088	0.080	0.360	5.760	0.077	0.009	-0.057	0.501	8.016
RAVEN	0.077	0.081	-0.130	0.265	4.240	0.081	0.069	-0.230	0.050	0.800	0.062	0.146	0.014	0.989	15.824
ROTATION	0.013	0.916	-0.112	0.499	7.984	0.033	0.725	-0.165	0.318	5.088	0.002	0.995	-0.039	0.814	13.024
SWM	0.095	0.114	-0.149	0.290	4.640	0.046	0.421	-0.106	0.463	7.408	0.125	0.047	-0.190	0.170	2.720
VWM1	0.086	0.004	-0.151	0.075	1.200	0.068	0.018	-0.185	0.031*	0.496	0.077	0.009	-0.102	0.229	3.664
VWM2	0.089	0.004	-0.156	0.066	1.056	0.076	0.010	-0.206	0.017*	0.272	0.077	0.009	-0.101	0.238	3.808
SUB	0.106	0.031	-0.172	0.122	1.952	0.064	0.154	-0.145	0.202	3.232	0.099	0.040	-0.168	0.133	2.128
COMSUB	0.083	0.072	-0.066	0.549	8.784	0.047	0.272	-0.077	0.493	7.888	0.081	0.078	-0.42	0.707	11.312
WORDM	0.082	0.007	-0.130	0.113	1.808	0.044	0.094	-0.078	0.351	5.616	0.093	0.003	-0.172	0.036*	0.576
PICTM	0.010	0.939	0.044	0.787	12.592	0.099	0.382	0.123	0.427	6.832	0.005	0.976	-0.031	0.853	13.648
EXCUT1	0.116	0.019	-0.232	0.041*	0.656	0.033	0.718	-0.138	0.398	6.368	0.106	0.029	-0.188	0.099	1.584
EXCUT2	0.094	0.012	-0.256	0.024*	0.384	0.103	0.032	-0.280	0.015*	0.240	0.107	0.028	-0.189	0.095	1.520
Number comparison	0.115	0.006	-0.074	0.445	7.120	0.071	0.058	-0.047	0.634	10.144	0.125	0.004	0.087	0.365	5.840
Visual tracing	0.107	0.010	-0.033	0.736	11.776	0.078	0.045	-0.092	0.363	5.808	0.110	0.009	0.030	0.764	12.224
Figure matching	0.120	0.005	-0.132	0.194	3.104	0.086	0.027	-0.143	0.169	2.704	0.116	0.006	-0.094	0.354	5.664
GO/NO GO	0.124	0.001	-0.200	0.032*	0.512	0.087	0.025	-0.137	0.153	2.448	0.164	0.000	-0.226	0.015*	0.240

Adjusted P (Bonferroni correction) = P values x compared times (16).
 CRT choice reaction time RAVEN Raven's Standard Progressive Matrices, ROTATION mental rotation, SWM spatial working memory, VWM1 verbal working memory, recite in order, VWM2 verbal working memory, recite in reverse order, SUB simple subtraction, COMSUB complex subtraction, WORDM word memory, PICTM picture memory, EXCUT1 executive function, same direction, EXCUT2 executive function, opposite direction, PVMMH periventricular white matter hyperintensity, DWMH deep white matter hyperintensity, P (F) P values with F test, β standardized coefficient.

*P values <0.05.

^aCognitive results were adjusted for age, sex, and education years.

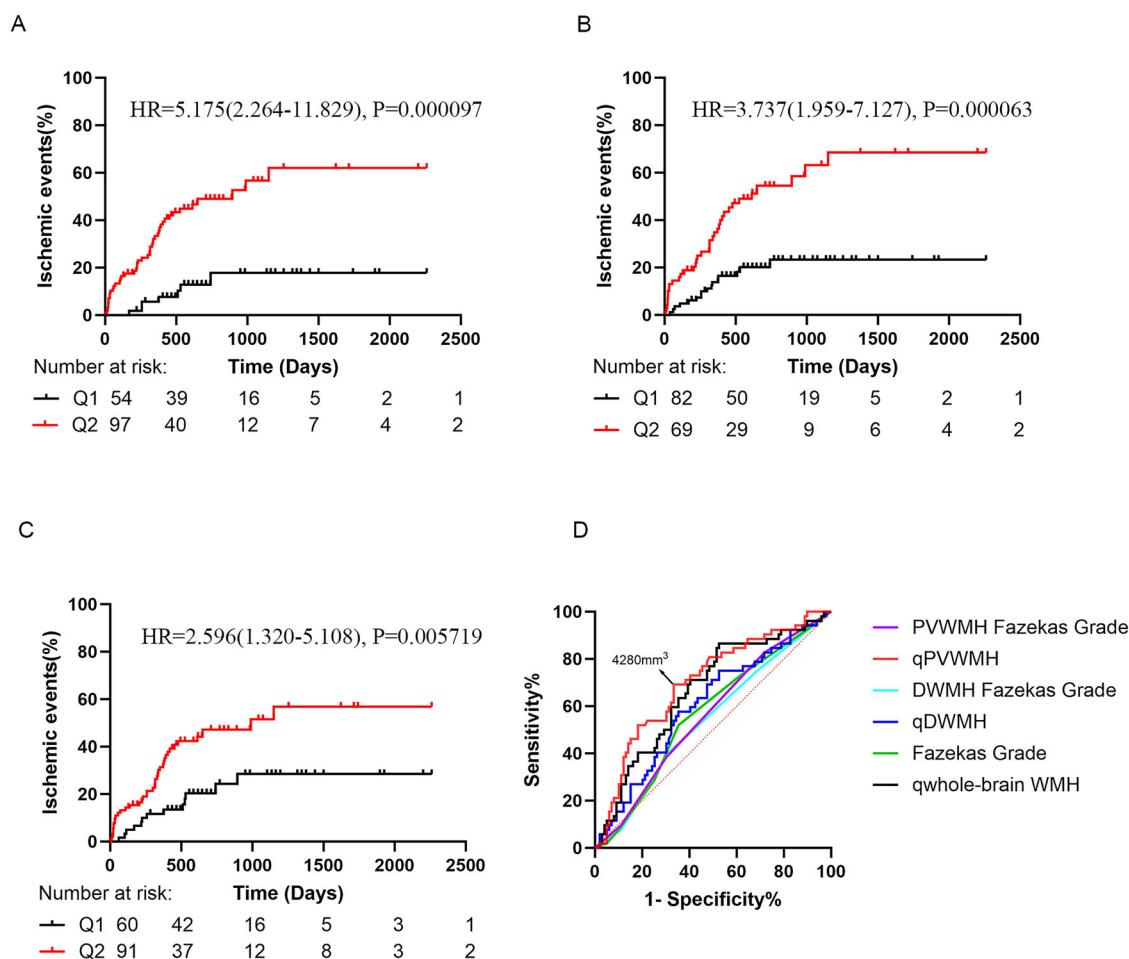


Fig. 2 | Cumulative incidence plots for ischemic events according to whole-brain, periventricular and deep WMHs in MMD patients. N = 151. A Ischemic events rate according to whole-brain WMHs. Black line (Q1): WMHs <6217 mm³; red line (Q2): WMHs ≥6217 mm³. **B** ischemic events rate according to the PVWMHs. Black line (Q1): WMHs <4280 mm³; red line (Q2): WMHs ≥4280 mm³. **C** ischemic events rate according to the DWMH. Black line (Q1): WMHs <2570 mm³; red line (Q2): WMHs ≥2570 mm³. **D** receiver operating characteristic (ROC) curves of

quantitative analysis compared with the Fazekas grade to distinguish ischemic events. The maximum Youden index occurred when the cutoff of the PVWMHs was 4280 mm³. MMD moyamoya disease, Q1 quartile 1, Q2 quartile 2, TIA transient ischemic attack, WMH white matter hyperintensity, q quantitative, PVWMH periventricular white matter hyperintensity, DWMH deep white matter hyperintensity.

information processing speed, executive function, visuospatial function, and verbal memory are lower in stroke-free patients with MMD than in normal controls⁸. Compared with general artificial cognitive evaluation methods such as the MoCA²⁶, our cognitive evaluation could be more objective with automatic grading, which reduces the subjective bias of experimenter artificial scoring. In addition, our study evaluated multiple cognitive domains with broad coverage in MMD patients.

Progressive stenosis or occlusion of the terminal internal carotid artery can lead to prolonged dilation of vessels such as the lenticulostriate artery and choroidal artery in MMD patients^{27,28}. These vessels can compensate for blood flow to a certain extent²⁹. However, owing to the fragility of these proliferative vessels, this compensatory mechanism may not be sufficient to prevent sustained silent ischemic injury³⁰. This “asymptomatic” ischemic injury most likely occurs first in the watershed region, which leads to cognitive decline. As the disease progresses, the number of collateral vessels gradually decreases, which may result in damage to the periventricular white matter microstructure¹³ and may account for the increased volume of PVWMHs in MMD patients. With the increase in WMHs in the whole brain, especially PVWMHs, simple calculation, verbal working memory, verbal memory, executive inhibition, and attention decreased linearly, whereas the effect of DWMHs was smaller. The periventricular white matter region may be an important region affecting specific cognitive domains.

Reduced blood perfusion due to left hemisphere involvement may be an important mechanism underlying intelligence and verbal working memory decline, and a decrease in executive inhibition is associated with bilateral hypoperfusion. A recent study revealed that executive function was associated with cerebral blood flow in the bilateral lateral frontal, centrum semiovale, and temporal lobes⁸. Low cerebral blood flow in the left centrum semiovale and temporal lobe is associated with decreased processing speed and verbal memory. Moreover, white matter microstructural damage was ameliorated to a certain extent after hypoperfusion was treated with revascularization. There were postoperative improvements in intelligence, organization, processing speed, and executive inhibition³¹. This result is consistent with the findings of our study. In patients with attention-deficit/hyperactivity disorder, the decreased efficiency of the right occipital node, together with abnormal connectivity to regions such as the anterior cingulate gyrus, may explain the attentional maintenance impairment³². After a right-hemisphere stroke, an abnormal pattern of functional connectivity between the right occipital lobe and the temporoparietal and inferior parietal lobes can lead to deficits in figure matching³³. Then, diminished connectivity between the right fusiform gyrus and the left superior occipital lobe leads to decreased performance on visuospatial tasks such as line bisection, reflecting the necessity of the occipital-parietal pathway in spatial working memory³³. In addition, decreased activation in the right occipitotemporal

Table 3 | Risk of ischemic events according to quantitative WMH volumes in MMD patients

	Unadjusted HR (95% CI)	P value	Adjusted HR (95% CI)	Adjusted P value*
Whole-brain WMHs (mm ³) ^a	6.570 (2.359–18.301)	0.000316	6.757 (2.274–20.075)	0.000585
Periventricular WMHs (mm ³) ^a	8.911 (3.227–24.610)	0.000024	8.824 (3.039–25.620)	0.000062
Deep WMHs (mm ³) ^a	2.578 (1.195–5.561)	0.015748	2.605 (1.144–5.929)	0.022529

HR hazard ratio, MMD moyamoya disease, WMH white matter hyperintensity.

*Adjusted for sex, education years, age, smoking, alcohol use, and comorbidities.

^aLog-transformed results.

region is associated with changes in visuospatial attention (N2pc component) in older individuals, suggesting the critical role of this region in age-related visual attention and working memory decline³⁴. Although the anatomical location is not very specific, the left frontal lobe plays an important role in executive control, executive inhibition, and simple calculation, whereas the left occipital lobe is involved in attention, executive inhibition and memory, and the right occipital lobe is associated with working memory and attention.

This study also has several limitations that must be acknowledged. First, long-term longitudinal cognitive data are lacking to further determine the causal relationship between cognitive dysfunction and WMH. Second, due to limited resources and time constraints, the number of healthy controls was smaller than that in the MMD group, and some factors (e.g., diabetes) were not exactly matched with those in the patient group, which may lead to heterogeneity between the two groups. Third, this study involved only the Chinese population, and as MMD is a relatively rare disease, the sample size was not very large. While the results are remarkable, it is important to note that good performance in a particular dataset does not guarantee generalizability. Further validation is needed in different datasets, multi-center and even transnational datasets. In addition, although the automatic WMH segmentation library UBO has been shown to be highly accurate in predicting WMH volumes, this study did not actually check the Dice scores or Hausdorff distances. In addition, modest HR values may have potential confounding factors, and this result needs to be viewed with caution. Finally, the brain MRI scans used in this study were high-resolution for research purposes. However, in the clinic, obtaining high-resolution MRI scans requires additional time and cost, making it relatively difficult to use quantitative measurements for risk assessment.

Conclusion

MMD patients without stroke retain most of their normal cognitive functions except for intelligence, mental rotation, spatial working memory, verbal working memory, and executive inhibition. With an increase in WMHs in the whole brain, especially PVWMHs, simple calculation, verbal working memory, verbal memory and attention functions decreased, whereas the effect of the DWMH increase was relatively limited. Increased WMHs in the left hemisphere were associated with decreases in intelligence and verbal working memory. An increase in PVWMHs, rather than DWMHs, could be an indicator of future ischemic events in MMD patients. Quantitative measurements of WMHs may be more accurate than qualitative measurements for predicting long-term ischemic events, and PVWMHs >4280 mm³ in MNI152 1 mm³ could be a potential cutoff value for further clinical decisions.

Data availability

The data that support the findings of this study are available from the authors, but restrictions apply to the availability of these data, which were used under license from Beijing Tiantan Hospital affiliated to Capital Medical University (Beijing) for the current study, and so are not publicly

available. However, the datasets generated during the current study are available from the corresponding author upon reasonable request. The source data for all figures and tables are available in Supplementary Data 1.

Received: 9 August 2024; Accepted: 24 June 2025;

Published online: 03 July 2025

References

- de Leeuw, F. E. et al. Prevalence of cerebral white matter lesions in elderly people: a population based magnetic resonance imaging study. The Rotterdam Scan Study. *J. Neurol Neurosurg. Psychiatry* **70**, 9–14 (2001).
- Lampe, L. et al. Lesion location matters: The relationships between white matter hyperintensities on cognition in the healthy elderly. *J. Cereb. Blood Flow Metab.* **39**, 36–43 (2019).
- Debette, S. et al. Association of MRI markers of vascular brain injury with incident stroke, mild cognitive impairment, dementia, and mortality: the Framingham Offspring Study. *Stroke* **41**, 600–606 (2010).
- Fazekas, F., Chawluk, J. B., Alavi, A., Hurtig, H. I. & Zimmerman, R. A. MR signal abnormalities at 1.5 T in Alzheimer's dementia and normal aging. *AJR Am. J. Roentgenol.* **149**, 351–356 (1987).
- Biesbroek, J. M. et al. Association between subcortical vascular lesion location and cognition: a voxel-based and tract-based lesion-symptom mapping study. The SMART-MR study. *PLoS ONE* **8**, e60541 (2013).
- Smith, E. E. et al. Correlations between MRI white matter lesion location and executive function and episodic memory. *Neurology* **76**, 1492–1499 (2011).
- Kang, C. G., Chun, M. H., Kang, J. A., Do, K. H. & Choi, S. J. Neurocognitive dysfunction according to hypoperfusion territory in patients with moyamoya disease. *Ann. Rehabil. Med.* **41**, 1–8 (2017).
- Shen, X. X. et al. Association of cognitive function and hypoperfusion in moyamoya disease patients without stroke. *J. Cereb. Blood Flow Metab.* **43**, 542–551 (2023).
- Liu, Z. et al. Association between white matter impairment and cognitive dysfunction in patients with ischemic moyamoya disease. *BMC Neurol.* **20**, 302 (2020).
- He, S. et al. Characteristics of cognitive impairment in adult asymptomatic moyamoya disease. *BMC Neurol.* **20**, 322 (2020).
- Yang, W. et al. Characteristics and clinical implication of white matter lesions in patients with adult moyamoya disease. *Neurology* **100**, e1912–e1921 (2023).
- Komatsu, K. et al. Reversibility of white matter hyperintensity by revascularization surgery in moyamoya disease. *J. Stroke Cerebrovasc. Dis.* **25**, 1495–1502 (2016).
- ten Dam, V. H. et al. Decline in total cerebral blood flow is linked with increase in periventricular but not deep white matter hyperintensities. *Radiology* **243**, 198–203 (2007).
- Kazumata, K. et al. Chronic ischemia alters brain microstructural integrity and cognitive performance in adult moyamoya disease. *Stroke* **46**, 354–360 (2015).
- Kazumata, K. et al. Combined structural and diffusion tensor imaging detection of ischemic injury in moyamoya disease: relation to disease advancement and cerebral hypoperfusion. *J. Neurosurg.* **134**, 1155–1164 (2020).
- Fujimura, M. et al. 2021 Japanese Guidelines for the Management of Moyamoya Disease: Guidelines from the Research Committee on Moyamoya Disease and Japan Stroke Society. *Neurol. Med. Chir.* **62**, 165–170 (2022).
- Zhou, X., Hu, Y., Yuan, L., Gu, T. & Li, D. Visual form perception predicts 3-year longitudinal development of mathematical achievement. *Cogn. Process.* **21**, 521–532 (2020).
- Wei, W. et al. Gender differences in children's arithmetic performance are accounted for by gender differences in language abilities. *Psychol. Sci.* **23**, 320–330 (2012).

19. Jiang, J. et al. UBO Detector - a cluster-based, fully automated pipeline for extracting white matter hyperintensities. *Neuroimage* **174**, 539–549 (2018).
20. Ashburner, J. A fast diffeomorphic image registration algorithm. *Neuroimage* **38**, 95–113 (2007).
21. Taylor, M. E. et al. White matter hyperintensities are associated with falls in older people with dementia. *Brain Imaging Behav* **13**, 1265–1272 (2019).
22. Zerna, C. et al. Association of white matter hyperintensities with short-term outcomes in patients with minor cerebrovascular events. *Stroke* **49**, 919–923 (2018).
23. Lai, P. M. R. et al. Asymptomatic moyamoya disease in a North American adult cohort. *World Neurosurg.* **161**, e146–e153 (2022).
24. Kuroda, S. et al. Five-year stroke risk and its predictors in asymptomatic moyamoya disease: Asymptomatic Moyamoya Registry (AMORE). *Stroke* **54**, 1494–1504 (2023).
25. Karzmark, P., Zeifert, P. D., Bell-Stephens, T. E., Steinberg, G. K. & Dorfman, L. J. Neurocognitive impairment in adults with moyamoya disease without stroke. *Neurosurgery* **70**, 634–638 (2012).
26. Nasreddine, Z. S. et al. The Montreal Cognitive Assessment, MoCA: a brief screening tool for mild cognitive impairment. *J. Am. Geriatr. Soc.* **53**, 695–699 (2005).
27. Velo, M. et al. Moyamoya vasculopathy: cause, clinical manifestations, neuroradiologic features, and surgical management. *World Neurosurg.* **159**, 409–425 (2022).
28. Kazumata, K. et al. Spatial relationship between cerebral microbleeds, moyamoya vessels, and hematoma in moyamoya disease. *J. Stroke Cerebrovasc. Dis.* **23**, 1421–1428 (2014).
29. Funaki, T. et al. Visualization of periventricular collaterals in moyamoya disease with flow-sensitive black-blood magnetic resonance angiography: preliminary experience. *Neurol. Med. Chir.* **55**, 204–209 (2015).
30. Yamashita, M., Oka, K. & Tanaka, K. Histopathology of the brain vascular network in moyamoya disease. *Stroke* **14**, 50–58 (1983).
31. Kazumata, K. et al. Brain structure, connectivity, and cognitive changes following revascularization surgery in adult moyamoya disease. *Neurosurgery* **85**, E943–E952 (2019).
32. Xia, S., Foxe, J. J., Sroubek, A. E., Branch, C. & Li, X. Topological organization of the “small-world” visual attention network in children with attention deficit/hyperactivity disorder (ADHD). *Front. Hum. Neurosci.* **8**, 162 (2014).
33. Ptak, R. et al. Discrete patterns of cross-hemispheric functional connectivity underlie impairments of spatial cognition after stroke. *J. Neurosci.* **40**, 6638–6648 (2020).
34. Lorenzo-Lopez, L. et al. Age-related occipito-temporal hypoactivation during visual search: relationships between mN2pc sources and performance. *Neuropsychologia* **49**, 858–865 (2011).

Acknowledgements

We thank Yehan Xiao for his contribution to this article. This study was supported by the National Natural Science Foundation of China (82171887)

and a Peking University International Hospital Research Grant (YN2022ZD04).

Author contributions

Z.L.: data curation, writing—original draft, writing—review and editing; X.H.: data curation, writing—review and editing; Q.D.: investigation, project administration; C.S.: software, methodology; H.L.: software, formal analysis; J.Z.: data curation; J.G.: visualization; S.H.: project administration; Y.W.: data curation; X.W.: data curation; Z.Z.: data curation; N.M.: resources; R.D.: conceptualization, supervision, validation, funding acquisition, project administration; X.Z.: supervision, validation; X.L.: formal analysis, supervision, methodology, visualization; R.W.: conceptualization, supervision, validation, funding acquisition, project administration.

Competing interests

The authors declare no competing interests.

Additional information

Supplementary information The online version contains supplementary material available at <https://doi.org/10.1038/s43856-025-00990-9>.

Correspondence and requests for materials should be addressed to Xin Lou or Rong Wang.

Peer review information *Communications Medicine* thanks the anonymous reviewers for their contribution to the peer review of this work.

Reprints and permissions information is available at <http://www.nature.com/reprints>

Publisher's note Springer Nature remains neutral with regard to jurisdictional claims in published maps and institutional affiliations.

Open Access This article is licensed under a Creative Commons Attribution-NonCommercial-NoDerivatives 4.0 International License, which permits any non-commercial use, sharing, distribution and reproduction in any medium or format, as long as you give appropriate credit to the original author(s) and the source, provide a link to the Creative Commons licence, and indicate if you modified the licensed material. You do not have permission under this licence to share adapted material derived from this article or parts of it. The images or other third party material in this article are included in the article's Creative Commons licence, unless indicated otherwise in a credit line to the material. If material is not included in the article's Creative Commons licence and your intended use is not permitted by statutory regulation or exceeds the permitted use, you will need to obtain permission directly from the copyright holder. To view a copy of this licence, visit <http://creativecommons.org/licenses/by-nc-nd/4.0/>.

© The Author(s) 2025